Electronic Supplementary Information

Plasmonic circular dichroism of vesicle-like nanostructures by template-less self-assembly of achiral Janus nanoparticles

Jia En Lu[a], Chou-Hsun Yang[b], Haobin Wang[b], ChiYung Yam[c], Zhi-Gang Yu[d,*], and Shaowei Chen[a,*]

[a] Department of Chemistry and Biochemistry, University of California, 1156 High Street, Santa Cruz, California 95064, USA

[b] Department of Chemistry, University of Colorado Denver, Denver, Colorado 80217, USA

[c] Beijing Computational Science Research Center, Haidian District, Beijing 100193, China

[d] Institute for Shock Physics and Department of Physics and Astronomy, Washington State University, Pullman, Washington 99164, USA

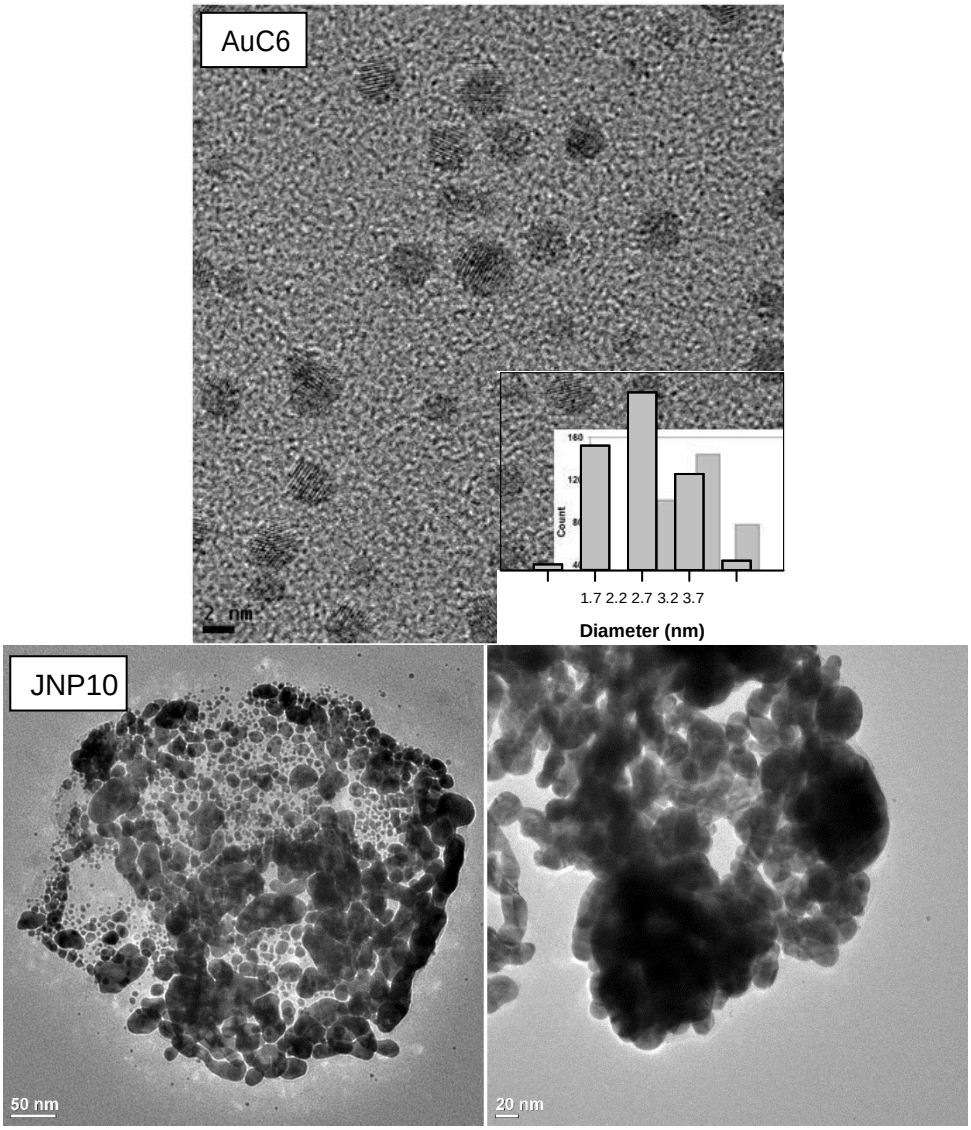

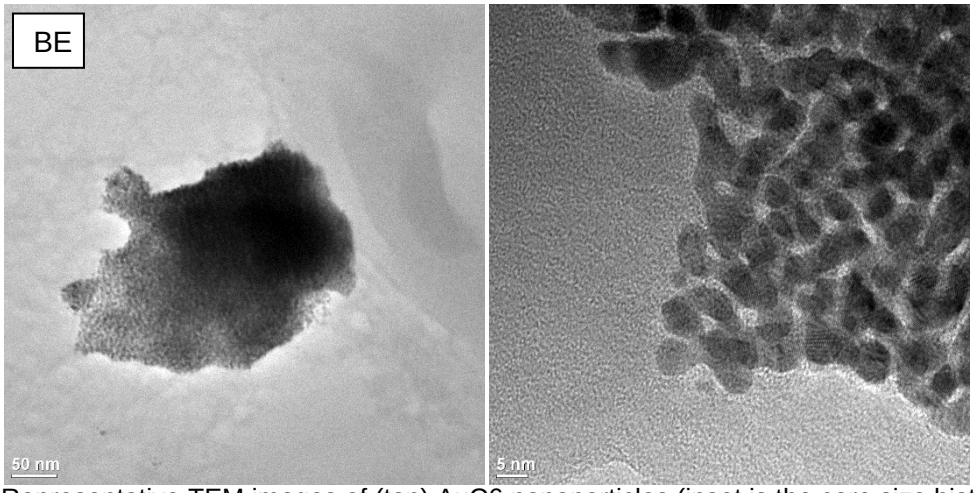

Figure S1. Representative TEM images of (top) AuC6 nanoparticles (inset is the core size histogram), (middle) JNP10 nanoparticles, and (bottom) BE nanoparticles. The last two samples were prepared at the nanoparticle concentration of 0.15 mg/mL.

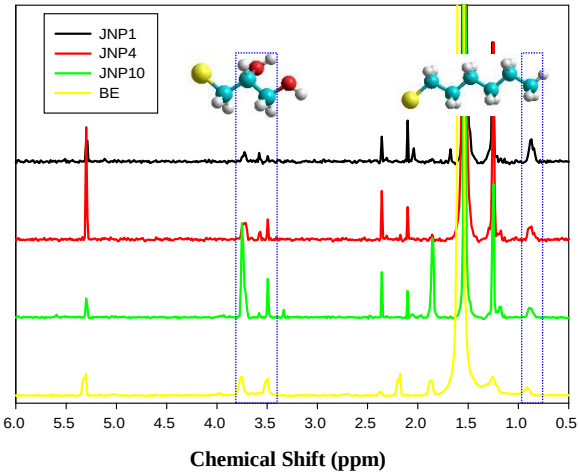

Figure S2. ^{1}H NMR spectra of AuC6-MPD JNP and BE nanoparticles in CD_2Cl_2. Based on the ratio of the integrated peak areas of the terminal C**H**$_3$ and -C**H**OH-C**H**$_2$OH protons (dotted boxes, as highlighted in figure insets), the MPD surface coverage was estimated to be 17.5 % for JNP1, 28.3 % for JNP4, 61.4 % for JNP10, and 66.0 % for BE nanoparticles.

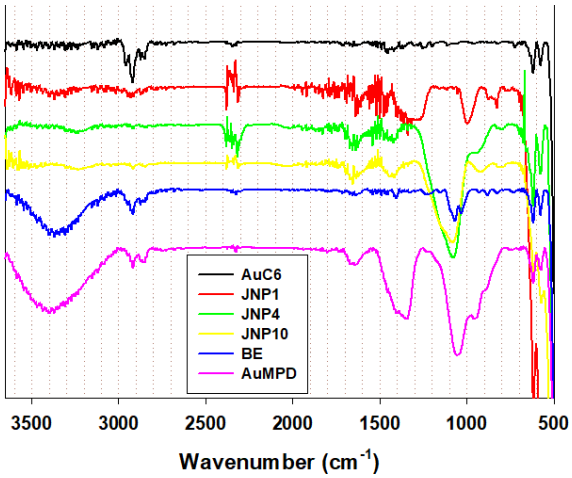

Figure S3. FTIR spectra of AuC6, JNP1, JNP4, JNP10, BE, and AuMPD nanoparticles.

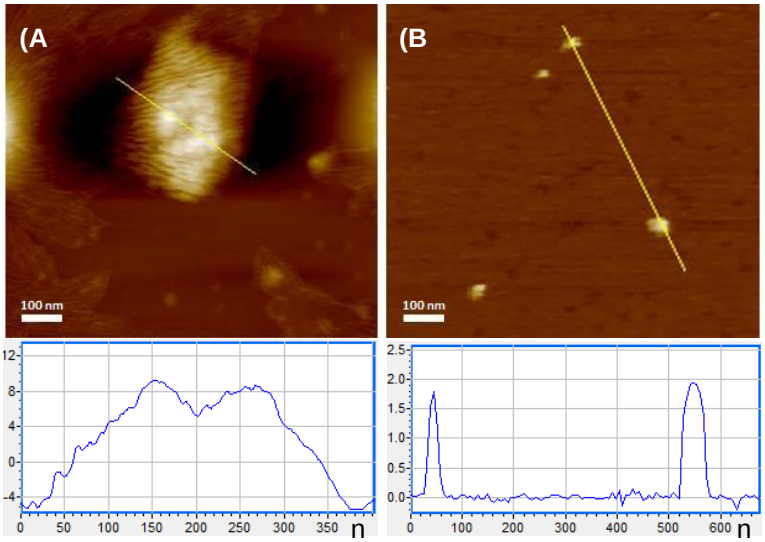

Figure S4. Representative AFM topographs of JNP10 nanoparticles at the concentrations of (a) 0.15 mg/mL and (b) 0.01 mg/mL in water. The bottom panels are the corresponding height profiles of the line scans in the top panels.

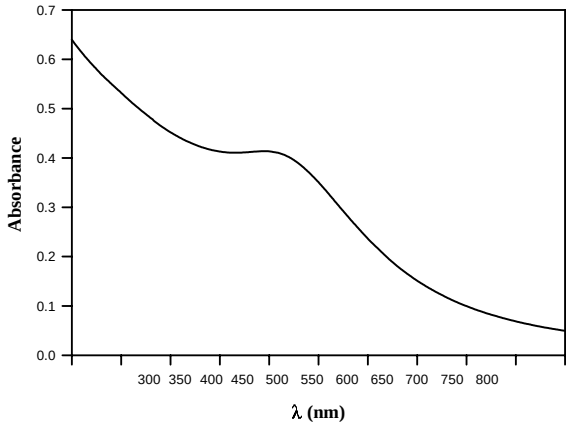

Figure S5. UV-vis absorption spectrum of AuC6 nanoparticles in $CHCl_3$.

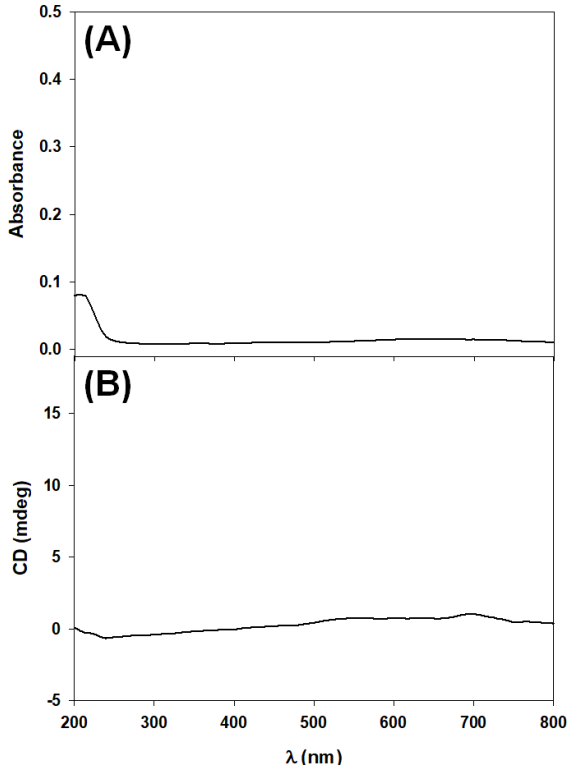

Figure S6. (A) UV-vis and (B) CD spectra of (racemic) MPD used in the present study at a concentration of 0.2 mM in water.

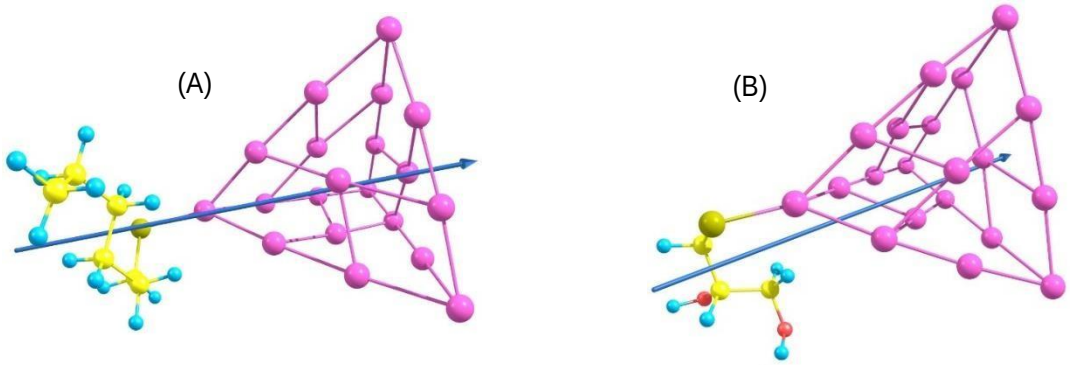

Figure S7. Transition dipole in a Au_{20} cluster capped with (A) C6 and (B) MPD. The excitation energies are 776 and 836 nm, respectively. It can be seen that adding ligands introduces directionality for the transition dipole moments.

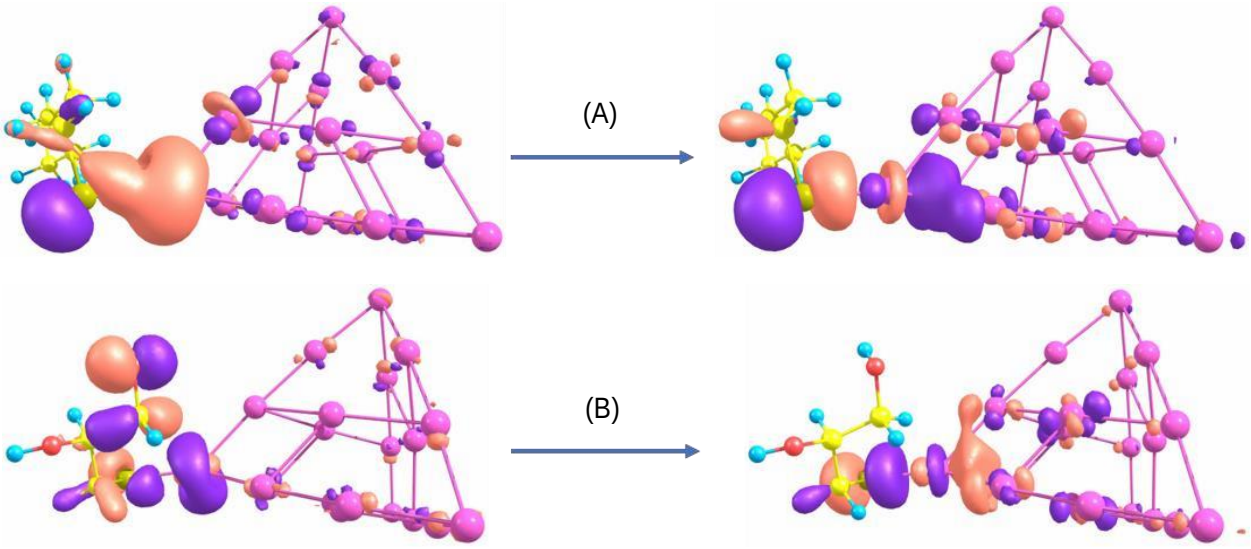

Figure S8. Transition of excited state in a Au_{20} cluster capped with (A) C6 and (B) MPD. The excited state transitions are visualized from molecular orbitals for the gold cluster linked with (A) one C6 and (B) one MPD, respectively. Both show that transitions occur approximately from ligand to gold cluster.

Furthermore, we studied the model with a Au_{20} Janus cluster capped with two different ligands. The transition dipole moment and transition of excited state are shown in Figure S9-S10. The excitation energy is 840 nm, and the direction of the transition dipole is from 3-mercapto-1,2-propanediol to the gold cluster.

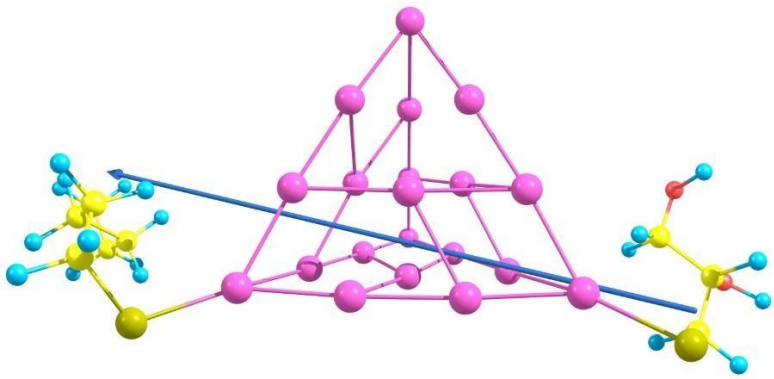

Figure S9. Transition dipole moment in a Au_{20} Janus cluster capped with C6 and MPD.

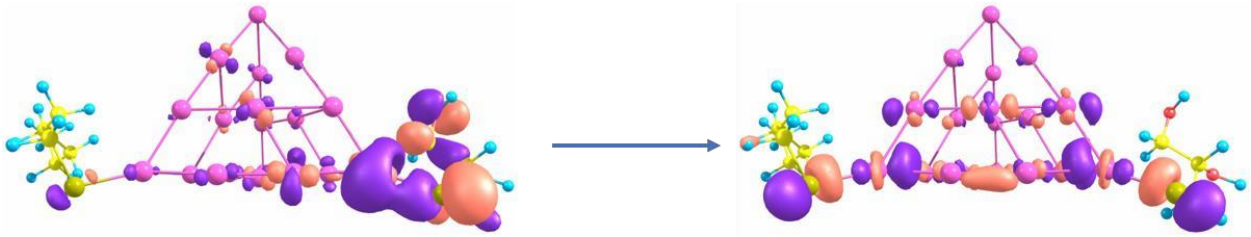

Figure S10. Transition of excited state in a Au_{20} Janus cluster capped with C6 and MPD.

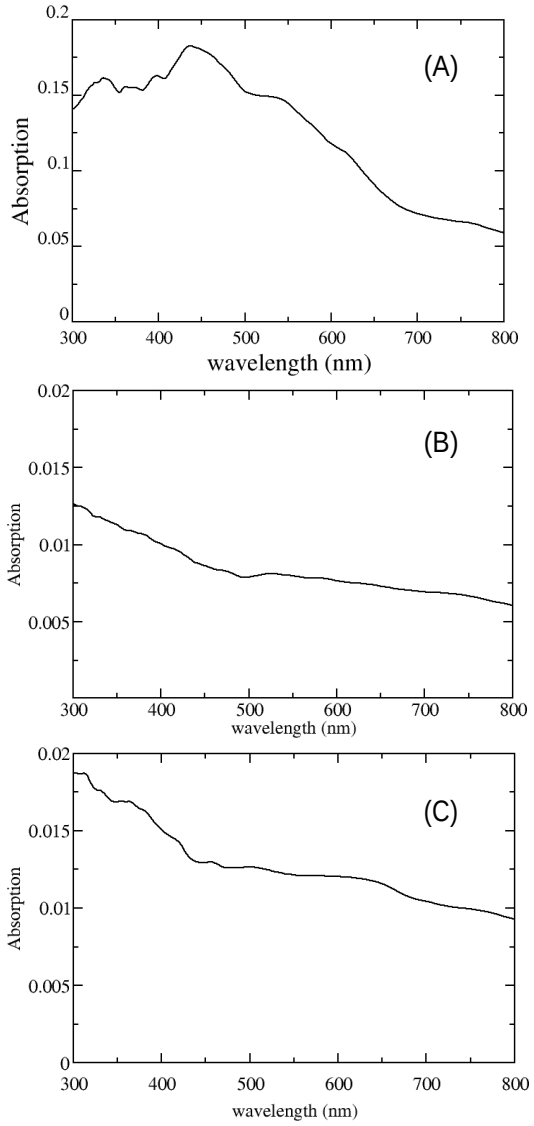

Figure S11. Absorption spectra with external field applied along the (A) x-axis, (B) y-axis, and (C) z-axis. From the calculations one can see that the absorbance is higher by an order of magnitude when the external field is applied along the x-axis (Scheme 1).